How to cite: *Angew. Chem. Int. Ed.* **2024**, *63*, e202412170
doi.org/10.1002/anie.202412170

Zeolites Synthesis

Stable Silica-Based Zeolites with Three-Dimensional Systems of Extra-Large Pores

Huajian Yu, Luis A. Villaescusa, Zihao Rei Gao, and Miguel A. Camblor**

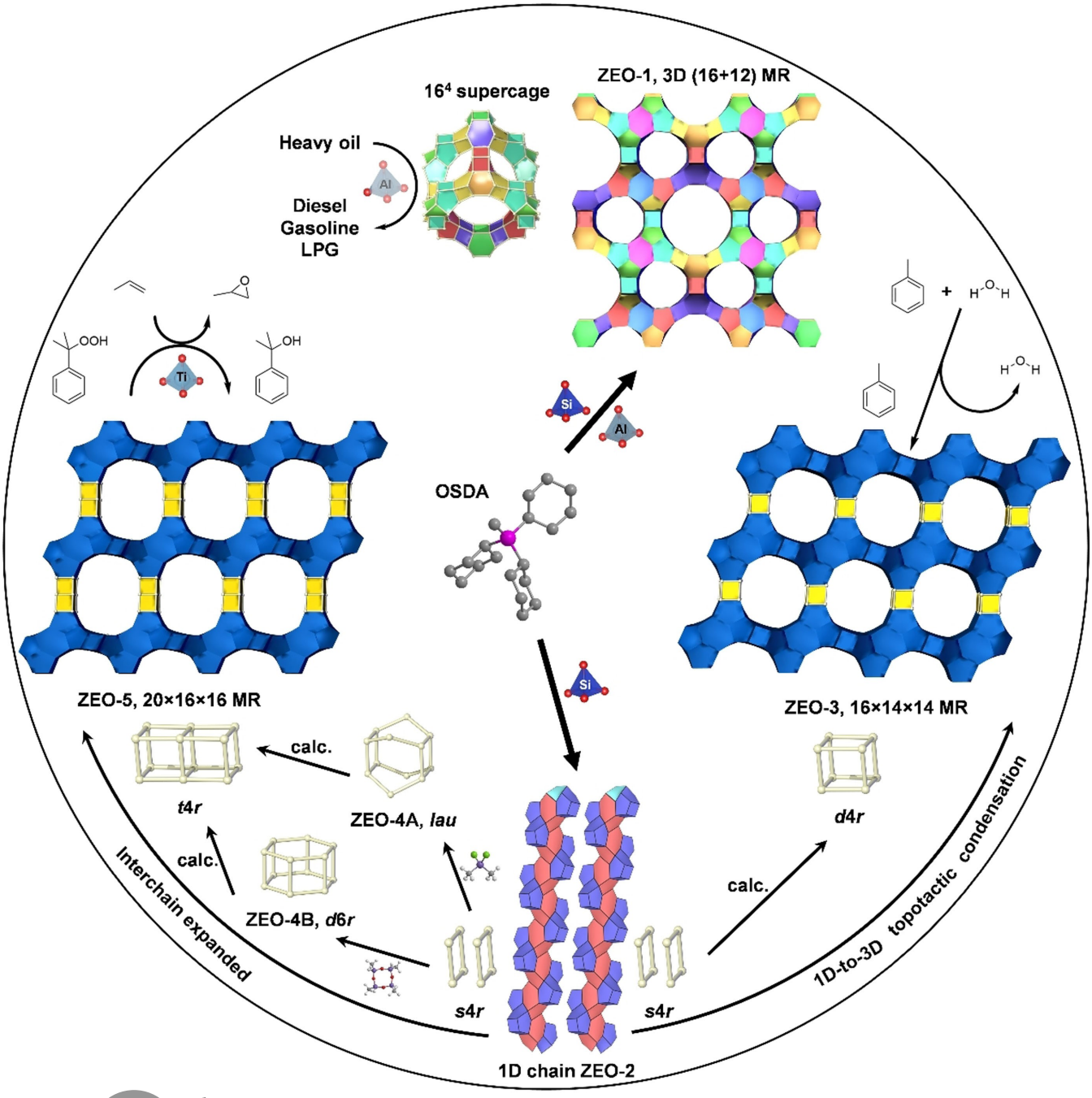

Abstract: Zeolites are microporous crystalline materials that find a very wide range of applications, which, however, are limited by the size and dimensionality of their pores. Stable silica zeolites with a three-dimensional (3D) system of extra-large pores (ELP, i.e., pores with minimum windows along the diffusion path consisting of more than 12 $SiO_{4/2}$ tetrahedra, 12R) are in demand for processing larger molecules than zeolites can currently handle. However, they have challenged worldwide synthetic capabilities for more than eight decades. In this review we first present a brief history of the discovery of ELP zeolites. Next, we show that earlier successes of zeolites with 3D ELP were not actually zeolites, but rather interrupted structures with, in addition, a composition that severely detracted from their stability. Finally, we present three new fully connected stable silica-based 3D ELP zeolites ZEO-1, ZEO-3 and ZEO-5, discuss their preparation methods and stability as well as the clear advantage of their increased porosity in catalysis and adsorption processes involving large molecules. We will discuss peculiar characteristics of their preparation and present two new reaction types giving rise to zeolites (1D-to-3D topotactic condensation and interchain expansion), highlighting how new synthesis methods can provide materials that would otherwise be unfeasible.

1. Introduction

Zeolites are crystalline microporous materials constructed from TB_4 tetrahedra that share their four vertices with neighboring tetrahedra once and only once, giving rise to a 3D framework which contains pores and/or cavities with the dimensions of small molecules. The Structure Commission of the International Zeolite Association currently recognizes 239 Zeolite Framework Types (ZFT) with unique topology, to which three-letter codes are assigned.[1] Several additional families of intergrowth zeolites exist and for some of them ordered polytypes have not been realized. Moreover, there are 17 additional "interrupted frameworks", which are not strictly zeolites (since not all the vertices are shared) and bear codes preceded by a hyphen. A typical zeolite can be constructed from SiO_4 tetrahedra but elements other than Si can occupy the center of the tetrahedra to some extent (T = Si, Al, Ge, P, Ti, B, Ga, Mg, Zn, Co, Be, etc) and elements different from O can also form the bridges (B = O, S, N, etc)[2]. The chemical composition, structure, crystal size and morphology, textural properties and even the T-atom ordering and framework flexibility of the zeolite all determine its physicochemical properties and performance in a given application.[3]

The wide structural and compositional variability of zeolites results in opportunities to fine-tune zeolites for specific applications, which include, among others, processes based on cation-exchange,[4] catalysis,[5] and adsorption.[6] Chemical modifications can even reverse properties and turn a natural zeolite from a cation exchanger into an anion trap for water purification.[7] All this variability is at the basis of the enormous commercial success of zeolites and continuously improves through advances in zeolite synthesis and modifications.[8] However, the pore size limits the size of the molecules that can access the inner zeolitic space where adsorption and catalysis take place. One of the most porous zeolites, the very successful catalyst with structure code **FAU**,[9] have pores around 7.4 Å free apertures (pore apertures are calculated from crystallographic data taking into account the van der Waals radius of O, 1.35 Å).

The dimensionality of the zeolite pore system is also of great importance. First, for a similar pore size, a higher dimensionality implies a higher porosity and an improved molecular diffusion,[10] Second, a higher dimensionality may impede pore clogging by byproducts or impurities in a treated stream.

So far, zeolite applications involving very large molecules have been hampered by the lack of stable zeolites displaying extra-large pores in three dimensions. Even if materials with possibly larger porosities, exemplified by mesoporous materials, like MCM-41,[11] and Metal–Organic Frameworks (MOFs), exist the intrinsically low catalytic activities of the former and a reduced stability of both the former and the latter[12] compared to zeolites result in limitations to their applicability. Stable zeolites with very large pores are, hence, in demand to process larger molecules, which is a topic of very high interest in several critical fields (energy, pollution, health, fine chemicals) related to a more sustainable world and a better use of resources. 3D ELP zeolites would facilitate the diffusion of bulky molecules, which are typically excluded from traditional microporous materials. This characteristic could enable the efficient catalysis of larger reactants, opening new pathways for chemical reactions that were previously

[*] H. Yu, Prof. M. A. Camblor
Instituto de Ciencia de Materiales de Madrid (ICMM), CSIC
c/ Sor Juana Inés de la Cruz 3, 28049 Madrid, Spain
E-mail: macamblor@icmm.csic.es
Dr. L. A. Villaescusa
Instituto Interuniversitario de Investigación de Reconocimiento Molecular y Desarrollo Tecnológico (IDM) Universitat de València–Universitat Politècnica de València
Camino de Vera sn, 46022, Valencia, Spain
and
CIBER de Bioingeniería Biomateriales y Nanomedicina (CIBER-BBN), 28029 Madrid, Spain
and
Departamento de Química, Universitat Politècnica de València, Camí de Vera sn, 46022, Valencia, Spain
Dr. Z. R. Gao
Department of Chemical and Biomolecular Engineering and Institute for NanoBioTechnology, Johns Hopkins University
Baltimore, MD, USA
E-mail: zgao44@jhu.edu

inaccessible. As a result, they would be particularly suited for applications in the petrochemical industry, where they could improve the efficiency of refining processes and the production of high-value chemicals, as well as for the production of biofuels and drugs. Larger pores could also find application for the removal and recovery/degradation of volatile organic compounds and of large persistent organic pollutants, which constitute a major concern nowadays because of their ubiquity and bioaccumulative, persistent and toxic character (frequently, carcinogenic, hepatotoxic and endocrine disruptors).[13] Cation exchange for the removal of charged organic pollutants, such as certain dyes and drugs, would also benefit from stable 3D ELP zeolites. Health applications could also be envisaged, for instance for drug delivery. Finally, there is also a fundamental interest in determining if there is an intrinsic and unavoidable limit to the porosity of zeolites.

In over 80 years of worldwide intensive zeolite synthesis research since the earlier works of Barrer and Breck,[14] only very recently stable zeolites with 3D systems of extra-large pores have been synthesized. The first 3D ELP zeolites reported were highly unstable and, then, essentially useless from the point of view of their potential applications (Table 1). Very recently, three new stable silica based 3D ELP zeolites have been prepared though three very different types of processes. The first one, ZEO-1, has been synthesized by a conventional hydrothermal approach with some less conventional features. The second one, ZEO-3, was prepared by an unprecedented 1D-to-3D topotactic condensation of a chain silicate. The last one, ZEO-5, is the result of an equally unprecedented interchain expansion zeolite reaction (IChEZ) of the same chain silicate. These works, which report successive zeolites with increasing porosity and the benefits they provide, collectively demonstrate that the porosity limit in zeolites had not yet been reached and that unexpected characteristics can be expected when unconventional procedures are undertaken. Furthermore, they bring the porosity limit in zeolites to the forefront, making it an open question worth investigating.

2. The quest for extra-large pores

2.1 Strategies

Historically, most ELP zeolites have been synthesized hydrothermally using organic structure directing agents (OSDA) which, in some extent, direct the crystallization. For the basis and history of hydrothermal synthesis, the reader is referred to the extensive review by Cundy and Cox.[14] Although alternative synthesis routes exist, such as ionothermal,[49] solvothermal,[50] and solvent-free syntheses,[51] hydrothermal synthesis continues to be the main route to zeolites. We will deal here only with the synthesis of ELP materials. Figure 1 shows the timeline of ELP zeolites, irrespective of dimensionality, composition or stability. The first ELP zeolite was reported in 1988: VPI-5 is an aluminophosphate zeolite with a 1D 18R pore (aperture of around 12 Å).[15] For the following 33 years, discovered ELP zeolites were either unstable 3D ELP (in red in Figure 1 and Table 1) or stable but with the extra-large pore just along one dimension (in black in Figure 1 and Table 1). So far, the different strategies for the synthesis of ELP zeolites heavily relied on the use of OSDA′s and/or

Huajian Yu obtained his bachelor's degree in Guangdong University of Technology in 2018 and his master's degree in South China Normal University in 2021. Currently, he is working in Instituto de Ciencia de Materiales de Madrid (ICMM–CSIC) for his PhD under Prof. Miguel A. Camblor's supervision. His research is mainly focused on the synthesis, structure characterization, modification and feasible potential applications of zeolite.

Luis Angel Villaescusa studied chemistry at the University of Valencia, Spain. He conducted his PhD at ITQ (Instituto de Tecnología Química) on directing structure strategies for the discovery of new zeolites under the guidance of Miguel Angel Camblor. After a two-year postdoctoral stay at the School of Chemistry in St. Andrews (Scotland), he received a 'Ramón y Cajal' fellowship to join the Department of Chemistry at the Universitat Politècnica de Valencia (UPV). There, he got a permanent position in 2011 as a senior lecturer.

Zihao Rei Gao gained his PhD degree in May 2022 under the supervision of Prof. Miguel A. Camblor in Materials Science Institute of Madrid (ICMM, CSIC) and currently is a post-doctoral fellow in Johns Hopkins University (JHU) working with Prof. Michael Tsapatsis. His research interest lies in the zeolite synthesis for new structures and/or novel features, structure characterization and topology study, and the modification of zeolites.

Miguel A. Camblor got his PhD in Chemistry from the Autonomous University of Madrid for work done at the Spanish National Research Council under the supervision of Prof. Pérez-Pariente. He has been a Fullbright Postdoctoral Fellow at Caltech and the head of the Research and Development Department of Industrias Químicas del Ebro. He is currently a Research Professor at the Institute of Materials Science of Madrid. His main interests are the discovery of new zeolite structures, their characterization and the exploration of possible uses.

Table 1: Extra-large pore Zeolites known to date[a].

Time[b]	$Ring_{max}$[c]	ZFT	Name	Type[d]	Pore System[e]	T	OSDA[f]	Solution[g]	Ref
1988	18	**VFI**	VPI-5	T,O	1D 18	Al P	N	PXRD	[15]
1990	14	**AET**	AlPO-8	T,O	1D 14	Al P	N^+	PXRD	[16]
1991	20	**-CLO**	Cloverite	I,O	3D (20+8)x(20+8)x(20+8)	Ga P	NH^+	SCXRD	[17]
1996	14	**DON**	UTD-1	T,O/D	1D 14	Si	M^+	TEM-PXRD	[18]
1997	14	**CFI**	CIT-5	T,O	1D 14	Si	N^+	PXRD	[19]
2001	14	**OSO**	OSB-1	T,O	3D 14x8x8	Si Be	–	SCXRD	[20]
2003	18	**ETR**	ECR-34	T,O	3D 18x8x8	Si Ga Al	N^+	PXRD	[21]
2003	14	**SFH**	SSZ-53	T,O	1D 14	Si B	N^+	PXRD	[22]
2003	14	**SFN**	SSZ-59	T,O	1D 14	Si B	N^+	TEM, MB, PXRD	[22]
2004	14	**UTL**	IM-12	T,O	2D 14x12	Si Ge	N^+	PXRD	[23]
2006	18	**ITT**	ITQ-33	T,O	3D 18x10x10	Si Ge	N^+	PXRD	[24]
2009	30	**-ITV**	ITQ-37	I,O	3D 30x30x30	Si Ge	N^+	SAED-PXRD	[25]
2010	18	**IRR**	ITQ-44	T,O	3D 18x12x12	Si Ge	N^+	PXRD	[26]
2010	16	**-IRY**	ITQ-40	I,O	3D 16x15x15	Si Ge	P^+	ED-PXRD, SCXRD	[27]
2011	28	**-IRT**	ITQ-43	I,O	3D 28x12x12	Si Ge	N^+	ADT-PXRD	[28]
2013	16	**IFO**	ITQ-51	T,O	1D 16	Al P Si	NH^+N	RED-PXRD	[29]
2014	21	**-EWT**	EMM-23	I,D	3D 21x10x10	Si (Al)	N^+	RED-PXRD	[30]
2014	18	-	NUD-1	T,O	3D 18x(12+10)x(12+10)	Si Ge	Im^+	SCXRD	[31]
2014	18	**-SSO**	SSZ-61	I,D	1D 18	Si	N^+	HRTEM-PXRD	[32]
2015	20	**-IFU**	ITQ-54	I,O	3D (20+8)x14x12	Si Ge	N^+	RED-PXRD	[33]
2015	15	-	GeZA	T,O	3D 15x12x12	Si Ge	S^+	PXRD	[34]
2015	14	**-IFT**	ITQ-53	I,O	3D 14x14x14	Si Ge	P^+	RED-PXRD	[35]
2016	14	-	CIT-13	T,D	2D 14x10	Si Ge	Im^+	RED-PXRD	[36]
2018	24	**-SYT**	SYSU-3	I,O	3D (24+8)x8x8	Si Ge	N^+	cRED-PXRD	[37]
2018	14	-	ECNU-9	I,O	2D 14x12	Si	-	MB, PXRD	[38]
2020	16	-	NUD-6	I,O	3D 16x8x8	Si (Al)	Im^+	SCXRD	[39]
2020	16	**-ION**	IDM-1	I,O	2D 16x10	Si	N^+	cRED-PXRD	[40]
2021	16	-	HPM-14	T,D	3D (16+8)x(9+8)x9	Si Ge	Im^+	cRED	[41]
2021	22	-	ITQ-56	I,O	3D 22x12x12	Si Ge	N^+	cRED-PXRD	[42]
2021	16	**JZO**	ZEO-1	T,O	3D (16+12)x(16+12)x(16+12)	Si Al	P^+	cRED-PXRD	[43]
2022	15	-	NUD-13	I,O	3D 15x12x12	Si Ge	Im^+	SCXRD	[44]
2022*	20	-	ITQ-70	I,O	3D 20x20x18	Si	P^+	EDT	[45]
2023	16	**JZT**	ZEO-3	T,O	3D 16x14x14	Si	-	cRED-PXRD	[46]
2024	20	-	ZEO-5	T,O	3D 20x16x16	Si	-	cRED-NPD-PXRD	[47]
2024*	24	-	ECNU-45	I,O	3D 24x10x10	Si	N^+	cRED-PXRD	[48]
2024*	24	-	ECNU-46	I,O	1D 24	Si	-	cRED-PXRD	[48]

[a] Stable 3D ELP zeolites in green, unstable 3D ELP zeolites in red and monodimensional ELP zeolite in black.
[b] Year of structural report (a * denotes a preprint or thesis).
[c] Number of tetrahedra in the window limiting diffusion along the widest pore.
[d] Character of the framework: T true zeolite (as opposed to interrupted framework), I interrupted framework, O ordered, D Disordered.
[e] Channel dimensionality and number of tetrahedra in the limiting window along each direction.
[f] type of OSDA used: N amine, NH^+ protonated amine, N^+ quaternary ammonium, M^+ metal complex. P^+ phosphonium, Im^+ imidazolium, NH^+N proton sponge, S^+ sulphonium. A hyphen means no OSDA was used (ECNU-9 was obtained through an interlayer expansion zeolite reaction, ILEZ reaction, ZEO-3 by a 1D-to-3D topotactic condensation, ZEO-5 by an IChEZ reaction and ECNU-46 by a thermal annealing of ECNU-45. No OSDA was used for the synthesis of **OSO**, according to the corresponding reference.
[g] Method used for the structural solution: SAED or ED ((Selected Area) Electron Diffraction), PXRD (Powder X-Ray Diffraction), ADT (Automated Diffraction Tomography), EDT (Electron Diffraction Tomography), cRED or RED ((continuous) Rotation Electron Diffraction), SCXRD (Single Crystal X-Ray Diffraction), HRTEM or TEM ((High-Resolution) Transmission Electron Microscopy), NPD (Neutron Powder Diffraction), and MB (Model Building).

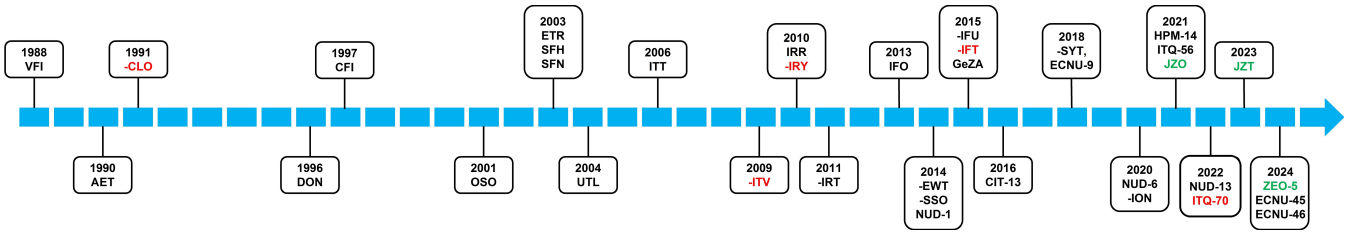

Figure 1. Timeline of the discovery of ELP zeolites. Color codes as in Table 1.

particular T-atom substitutions. Ammonium, amine, phosphonium, proton sponge, sulphonium and metal complex have all been used as structure-directing agents in the synthesis of ELP zeolites (Table 1). However, the most porous materials, containing interconnected ELP required also the introduction of heteroatoms. In particular, the use of Ge favors the formation of *d*4*r* (or even *d*3*r*)[52] because Ge(IV) is more ionic and have longer Ge–O bond length and more flexible O–Ge-O bond angle compared to Si(IV), so it releases the strain associated to those units. F^- also helps in stabilizing *d*4*r* by incorporation into it and increasing the ionicity of the T–O bond.[53] The importance of building units with small rings (*d*4*r*, *d*3*r*) lies in their unique topological contribution which can result in a decrease of framework density.[54]

2.2 The stability problem

Most known multidimensional ELP zeolites have a poor stability, mainly because of their composition. In fact, half of the zeolites in Table 1 are germanosilicates or berilosilicates of poor stability. Germanosilicates with high Ge content typically collapse during or after calcination followed by exposure to non-dried air. First, a carboreduction of Ge may occur during calcination.[55] Second, once calcined, the ability of Ge to increase its coordination above 4 and the longer and more ionic and labile character of the Ge–O bond compared to the Si–O bond, favors a hydrolytic attack.[56] This can sometimes be solved by replacing Ge by other atoms through post-synthetic procedures.[57] It can even be exploited to produce new zeolites through the assembly-disassembly-organisation-reassembly (ADOR) process,[58] a method that converts certain unstable germanosilicates into more stable silicates with a different topology but with smaller pores or at most the same size as the parent.[59] Anyway, the stability issue is clearly an inconvenience of the germanosilicate strategy to ELP zeolites. With regard to berilosilicate OSB-1, its very low stability can be attributed to the high charge density of the $[BeO_{4/2}]^{2-}$ tetrahedron and the fact that the pore walls are made of single 3-rings without crosslinkings.[20] In our opinion chemical composition is likely more important than framework connectivity completeness as illustrated by the cases of **-EWT**, **-SSO**, ECNU-9, and **-ION**. All these silica-based interrupted frameworks show pretty good stabilities, withstanding calcination to free the pore space and even temperatures up to 1000 °C in the case of **-ION**.[40] That is not the case for NUD-6 despite its silica-based composition most likely because this interrupted framework contains neighboring Q^3 pairs.

Concerning specifically 3D ELP zeolites, only **-CLO**, **-ITV**, **-IRY**, and **-IFT** were known until recently, all interrupted frameworks rather than true zeolites. Materials with these structures have been realized only with a composition contributing to their instability (galliumphosphates or germanosilicates). Additionally, interrupted structures typically contain dangling T-OH bonds pointing into the channels and are often lobed rather than exhibiting an ample free aperture, both factors reducing the effective pore openings (except for **-IRY**).

3. Stable 3D ELP zeolites

3.1 Conventional hydrothermal synthesis of ZEO-1

The first silica based 3D ELP zeolite, ZEO-1 (**JZO**),[43] was prepared by a conventional hydrothermal route that incorporated two somehow less conventional characteristics that proved to be very important. First, the OSDA used was a pretty large phosphonium cation, tricyclohexylmethylphosphonium (Cy_3MeP^+). Second, the synthesis temperature, 190 °C, was pretty high compared to most standard zeolite crystallizations, which suggests the crystallization of ZEO-1 has a high overall activation energy. Phosphonium cations have been used before in zeolite synthesis but, by themselves, they did not produce silica-based 3D ELP. Interrupted 3D ELP zeolites **-IRY** and **-IFT** (Table 1) require the use of Ge for their crystallization in addition to a phosphonium OSDA and are unstable after calcination upon contacting ambient air.[27,35] This is also the case for ITQ-70.[45] Up to our knowledge Cy_3MeP^+ had never been reported as a successful OSDA in zeolite synthesis. There are two factors that are important with regard to the use of phosphonium cations. First, as P is bigger than N it may afford larger substituting groups, leading to somehow larger cations than similar alkylammonium cations. Second, phosphonium cations are also more stable in hydrothermal alkaline conditions,[60] which allows Cy_3MeP^+ to withstand the long crystallization at 190 °C (15–30 days) even in hydroxide media (although ZEO-1 was initially discovered using fluoride, it can be also synthesized by the hydroxide route).

With a unit cell volume of >46900 Å^3 and 21 Si plus 43 O in the asymmetric unit, the structure of ZEO-1 is one of the most complex crystal structures solved among zeolites (Figures 2E, 2F). It was solved using cRED data obtained from minute crystals (<200 nm), confirming the extraordinary power of this technique, then refined by the Rietveld method using synchrotron PXRD data. It contains a very complex system of pores: 16R extra-large pores plus 12R large pores along the three dimensions (along *c*-axis the pores are sinusoidal). Since all those pores are interconnected, three types of supercages arise in the intersections: one with access through four 16R, another through two 16R plus two 12R and the last one with access only through four 12R (Figures 2A–C, respectively, compared to **FAU** supercage in 2D).

This very open structure translated into a then record surface area of around 1000 $m^2 g^{-1}$ (Table 2), allowing ZEO-1 to adsorb over 40 times as much Nile Red as ultra-stable Y zeolite (**FAU**), showing thus potential for decontamination (Figure 3A). It also proved superb as a catalyst for the fluid catalytic cracking of heavy oil, increasing the yield of gasoline, diesel and liquified petroleum gas (Figure 4A).

The synthesis of this complex structure with different pores and different supercages with a single Cy_3MeP^+ cation

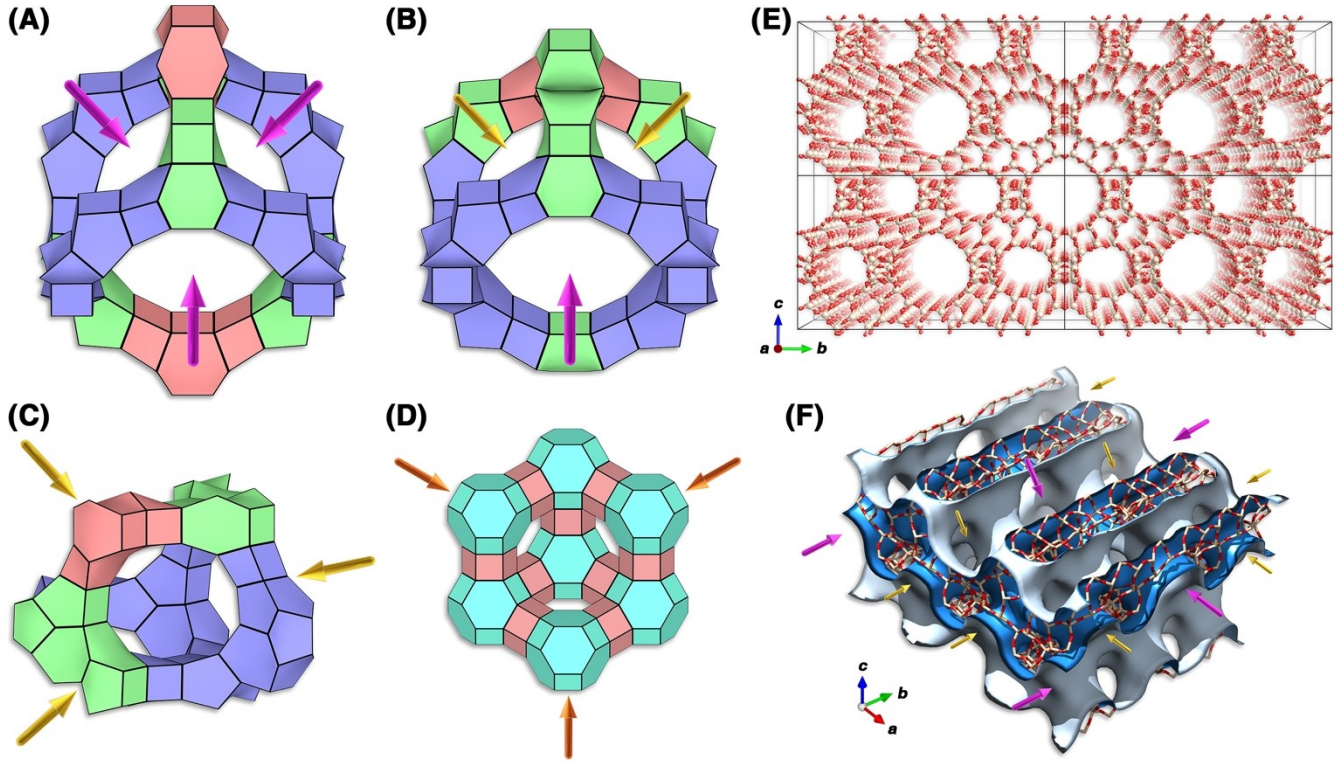

Figure 2. ZEO-1 has an extraordinary porosity of crossing 3D extra-large and large pores that give rise to three different types of "supercages" with entrances through four 16R (A), two 16R and two 12R (B) and four 12R windows (C). The supercage of **FAU** (D) is shown for comparison. The large difference in size between the extra-large and large pores is evident in the perspective view on (E) and the 3D pore model in (F). Modified from reference[43] with permission, copyright © 2021 The American Association for the Advancement of Science.

Table 2: The textural properties of ZEO-1, -3, -4A, -4B, -5A and 5B derived from Ar adsorption.

	BET area (m^2/g)	Pore volume (cm^3/g)	Pore size distribution (Å)
ZEO-1	1037	0.347	6.7/7.9/11.5
ZEO-3	1032	-	8.8/10.8
ZEO-4A	687	0.249	7.9/10.0/10.9/13.0/15.5
ZEO-4B	841	0.299	8.7/10.0/10.9/12.5
ZEO-5A	1533	0.399	10.0/11.5/16.7
ZEO-5B	1832	0.382	10.0/11.5/16.7

cannot be considered anything close to a "template effect" in the sense of a key-lock correspondence[61] (unless different conformations stabilize the very different supercages, which is unlikely) making the driving force for its crystallization intriguing. ZEO-1 continues to be the only 3D ELP aluminosilicate and it is stable up to at least 1000 °C. Its physicochemical properties have been investigated in detail recently.[62]

3.2 1D-to-3D topotactic condensation: ZEO-3

When the synthesis of ZEO-1 is attempted without aluminium at 175 °C a 1D chain silicate, ZEO-2, is formed instead of a zeolite.[46] This chain silicate (Figures 5A, 5 C) is zeolitic in the sense that it is embedded in the structure of polymorph B of the large pore zeolite Beta (see below), where it connects with neighboring chains by sharing single 4-rings, *s4r*.[63] In ZEO-2 neighboring chains are connected through hydrogen bonds between silanols (Figure 5D) in these *s4r* (Figure 5B). However, when ZEO-2 is calcined an unprecedented 1D-to-3D topotactic condensation occurs transforming the chain silicate into a new zeolite, ZEO-3 (Figures 5F–G). The connection between chains is made through the *s4r* so *d4r* units are created (Figure 5E) with elimination of Q^3 (Figure 5H). Hence, all the pores in ZEO-3 (16x14x14R) are larger than those in zeolite Beta (12x12x12R). This transformation, which has been likened to the Nobel Prize winning "click chemistry",[64] is topotactic because the topology of the chain is preserved. This is the first example of a *d4r* unit in a pure silica zeolite prepared without the aid of fluoride anions.[65] Formally, ZEO-3 can be considered the σ-expansion of polymorph B of Beta, Figures 6A–B, 6D–E and 6G–H (in a σ-expansion new nodes are introduced by expanding the net along planes, which is the same formal relation between $AlPO_4$-5 and VPI-5).[15] It was hypothesized that a chiral ELP zeolite could be prepared from the analogous chain silicate embedded in the chiral polymorph A of Beta.

The structures of ZEO-2 and ZEO-3 were also solved from cRED data and refined against synchrotron PXRD, and the structures were confirmed by high-resolution

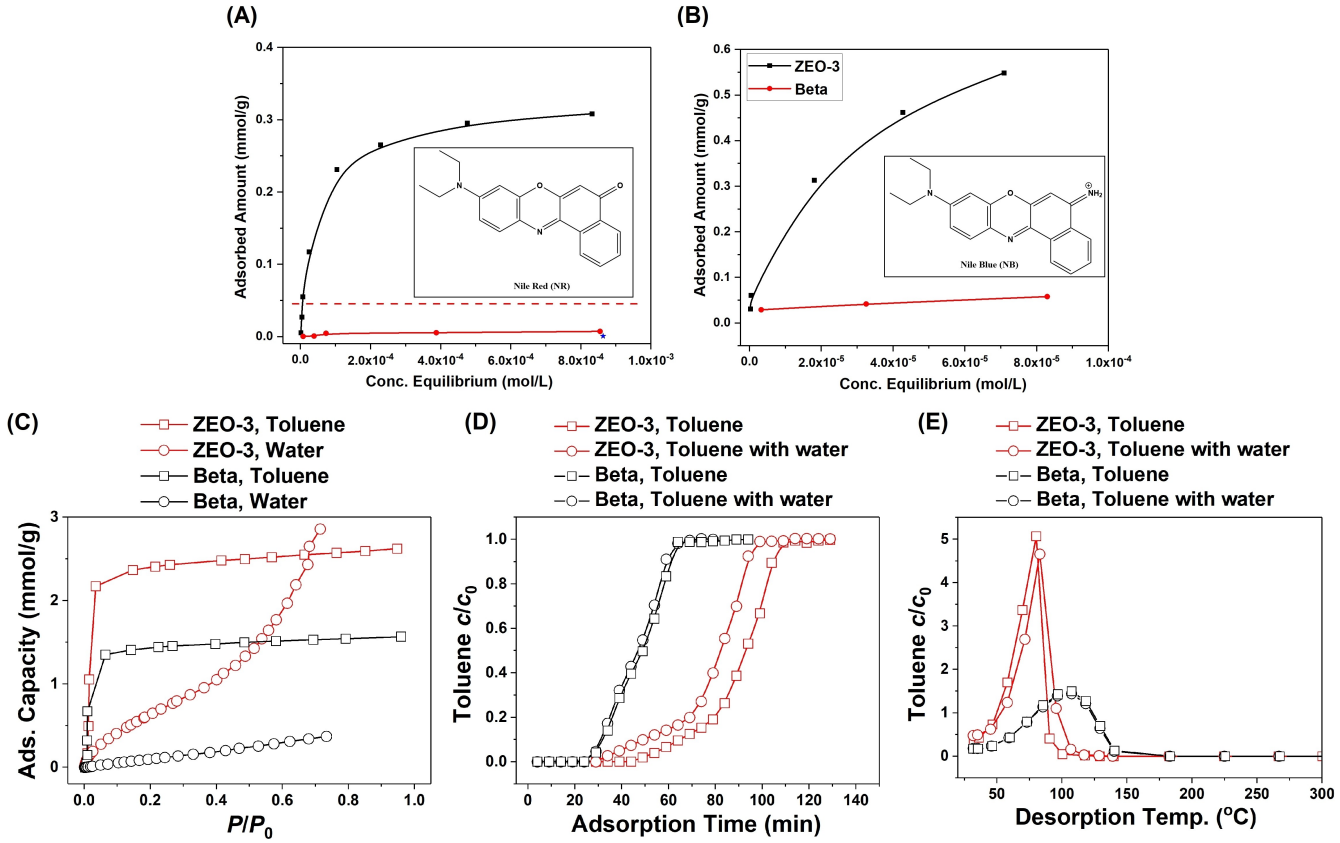

Figure 3. Extra-large pore zeolites can find applications as adsorbents for decontamination. ZEO-1 can adsorb over 40 times more Nile Red than 3D large pore USY (dealuminated **FAU**) (A). Similarly, ZEO-3 adsorbs much more Nile Blue than pure silica 3D large pore Beta (B). Also, ZEO-3 outperforms silica Beta in the removal and recovery of toluene, as a model for a VOC (C–E). Not only ZEO-3 adsorbs more VOC (C) but the breakthrough curves clearly show a higher retention even in the presence of water (D). Furthermore, the toluene recovery temperature is lower in ZEO-3 than in Beta (E). Modified from references[43] and[46] with permission, copyright © 2021 and 2023 The American Association for the Advancement of Science.

scanning transmission electron microscopy (HRSTEM). The porosity of ZEO-3 is similar to that of ZEO-1 (Table 2) and its pure silica composition allows it to adsorb a large amount of Nile Blue from solution (Figure 3B) and also the removal and recovery of volatile organic compounds (VOC) from a gas stream, suggesting potential in decontamination processes. ZEO-3 behaved similarly to UiO-66 for VOC removal while outperformed this MOF when successive cycles of adsorption and regeneration were realized because of its better stability. This highlights the importance of the higher stability of zeolites even in applications under no very harsh conditions (<400 °C). ZEO-3 is in fact stable to calcination up to at least 1100 °C in air or 760 °C in 10 % humidity.[46] Also, recovery of the VOC was achieved at a lower temperature in the case of ZEO-3 (Figures 3C–E). Although it was possible to introduce small amounts of Ti into ZEO-2 by direct synthesis, both tetrahedral and octahedral Ti were found in ZEO-3, what would in principle detract from its use in catalysis. Thus, further optimization work is required.

3.3 Interchain expansion and condensation: ZEO-5

In view of the structure of the chain silicate ZEO-2 (Figure 7a), the possibility was stablished to go one step further and try to connect the chains with a silane rather than connecting them directly. Two different silanes were tried, dichlorodimethylsilane (DCDMS) and 2,4,6,8-tetramethylcyclotetrasiloxane (TMCTS) both resulting in two new interrupted frameworks with extra-large pores (20x16x16R): ZEO-4A and ZEO-4B (Figures 7b-c), respectively.[47] While Inter-Layer Expansion reactions have been known for years,[66] this is the first report of an InterChain Expansion Zeolite Reaction (IChEZ). The difference between ZEO-4A and -4B lies on the newly introduced Si atoms: in ZEO-4A they contain two dangling methyl groups, while in ZEO-4B they only contain one and are connected between them in pairs (which implies TMCTS is broken in the acidic medium used for the reaction). Amazingly, after calcination both interrupted frameworks transformed into the same fully connected SiO_2 zeolite, ZEO-5 (Figure 7d), through complete condensation of the newly introduced Si atoms with transformation of known *lau* and *d6r* units (Figures 6J–K respectively) into a new type of

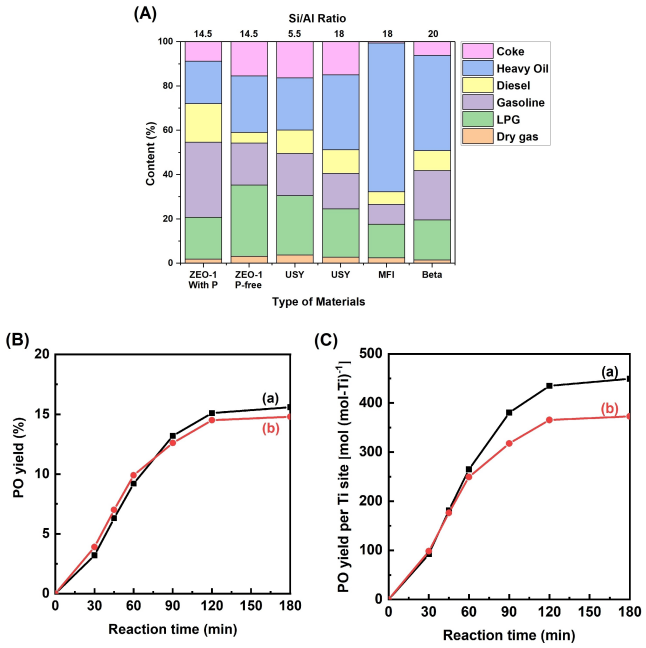

Figure 4. Catalysis. ZEO-1 (A) converts by catalytic cracking more heavy oil and produces more LPG, gasoline and diesel than commercial catalysts. Ti-ZEO-5, despite its microporous nature, shows a similar performance in the epoxidation of propylene by the cumene hydroperoxide route as the mesoporous Ti-HMS (B), as well as a higher intrinsic activity of Ti (C). Modified from reference[43] with permission, copyright © 2021 The American Association for the Advancement of Science (A) and reference[47] (B and C).

structural unit, a triple 4-ring, *t4r* never observed before in any type of zeolite (Figure 7).[47]

Contrary to the 2D-to-3D ILEZ generally yielding interrupted structures with Q^3 Si at the expansion sites, the 1D-to-3D IChEZ expansion plus topotactic condensation results in ZEO-5, which is a fully connected framework.

The structures of ZEO-4A and -4B and ZEO-5 were solved by cRED and refined against synchrotron PXRD data (Table 3). In the case of ZEO-5, given its extraordinary characteristics and because of some concerns from the referees, a combined refinement using cRED, synchrotron PXRD and neutron powder diffraction data was undertaken. The structures of the three materials were confirmed by HRSTEM.

In both ZEO-4A and ZEO-4B interrupted organozeolites the pores are lobed and contain dangling Si-CH_3 protruding into the channel so the measured BET areas (Table 2), while being larger than those of typical zeolites, don't reach the values of ZEO-1 and ZEO-3. However, after the condensation reaction the newly introduced Si get full connectivity, becoming all Q^4 Si sites and providing ZEO-5 with a wider clearance of the pores and an extraordinary porosity that breaks the previous record held by ZEO-1 (Table 2). Interestingly, despite being a condensation reaction, the transformation of ZEO-4A and ZEO-4B into ZEO-5 leads to a significant expansion of the framework (12 and 7.6 %, respectively). This occurs along the *a*- and *b*- axes and is mainly due to the change in the structural unit from the "pudgy" *lau* and *d6r* units to the more svelte and elongated *t4r*. As with the 1D-to-3D condensation discussed above in 3.2, this interchain expansion-condensation is also topotactic, as the topology of the chain remains invariant. It is interesting to remark that ZEO-5 represents the first real rather than virtual σ-expansion from ZEO-3 (Figures 6B–C, 6E–F, 6H–I), since new Si nodes have been actually introduced by a silylation reaction.

ZEO-5 is the oxide true zeolite of lower framework density (FD = 11.07 Si nm^{-3}) with a calculated density of 1.10 g cm^{-3}. Among ZFT structures recognized by the IZA only **RWY** (a very unstable Ga, Ge chalcogenide) has a lower FD of 7.6. Other ZFT corresponding to oxides and close to ZEO-5's FD are **-IRY** (11.1) and **-ITV** (10.5), both unstable germanosilicates with interrupted frameworks. Because of their composition, all these three materials present a density above ZEO-5, which is then the lighter zeolite reported ever. Despite this low density and the strain inherent to the *t4r* unit, which pushes ZEO-5 to the assumed energetic limit of realizable zeolites,[67] once prepared ZEO-5 can withstand calcination up to at least 1000 °C and steaming at 760 °C under 10 % H_2O. The ^{29}Si MAS NMR of ZEO-5 is interesting because it shows a resonance at −98.6 ppm, which despite its very low field, more typical of Q^3 or even Q^2 in zeolites, is actually a Q^4 with very acute Si-O–Si angles. This resonance was assigned to the Si in the central ring of the *t4r* (average angles around 137°) and DFT calculations support the assignment. Interestingly, old empirical correlations between structural parameters and chemical shifts failed to properly account for this resonance (the average Si-O–Si angles for the Si atoms in the central ring would resonate at −104 ppm according to the equation by Thomas et al.)[68] likely due to the limited dataset used to establish the correlation. By contrast, a more modern correlation including a larger (DFT-optimized) dataset and

Table 3: Crystallographic data of the materials discussed in this minireview.

	Unit Cell					Crystal system	Space group
	a	*b*	*c*	*β*	Volume		
ZEO-1	43.4612(6) Å	43.4612(6) Å	24.9754(8) Å	90°	47175(2)Å^3	Tetragonal	$I4_1/amd$
ZEO-2	23.5465(7) Å	24.7446(7) Å	14.4024(4) Å	115.1974(9)°	7593.0(4) Å^3	Monoclinic	*C*2/*c*
ZEO-3	21.5046(8)Å	21.2757(8)Å	14.4638(4)Å	108.7196(15)°	6267.5(4) Å^3	Monoclinic	*C*2/*c*
ZEO-4A	25.349(3) Å	21.783(3) Å	14.3492(6) Å	102.300(4)°	7741.5(14)Å^3	Monoclinic	*C*2/*c*
ZEO-4B	25.879(2) Å	22.696(2) Å	14.3528(3) Å	106.983(2)°	8062.4(10)Å^3	Monoclinic	*C*2/*c*
ZEO-5	25.278(4) Å	24.665(4) Å	14.4173(7) Å	105.244(4)°	8673(2)Å^3	Monoclinic	*C*2/*c*

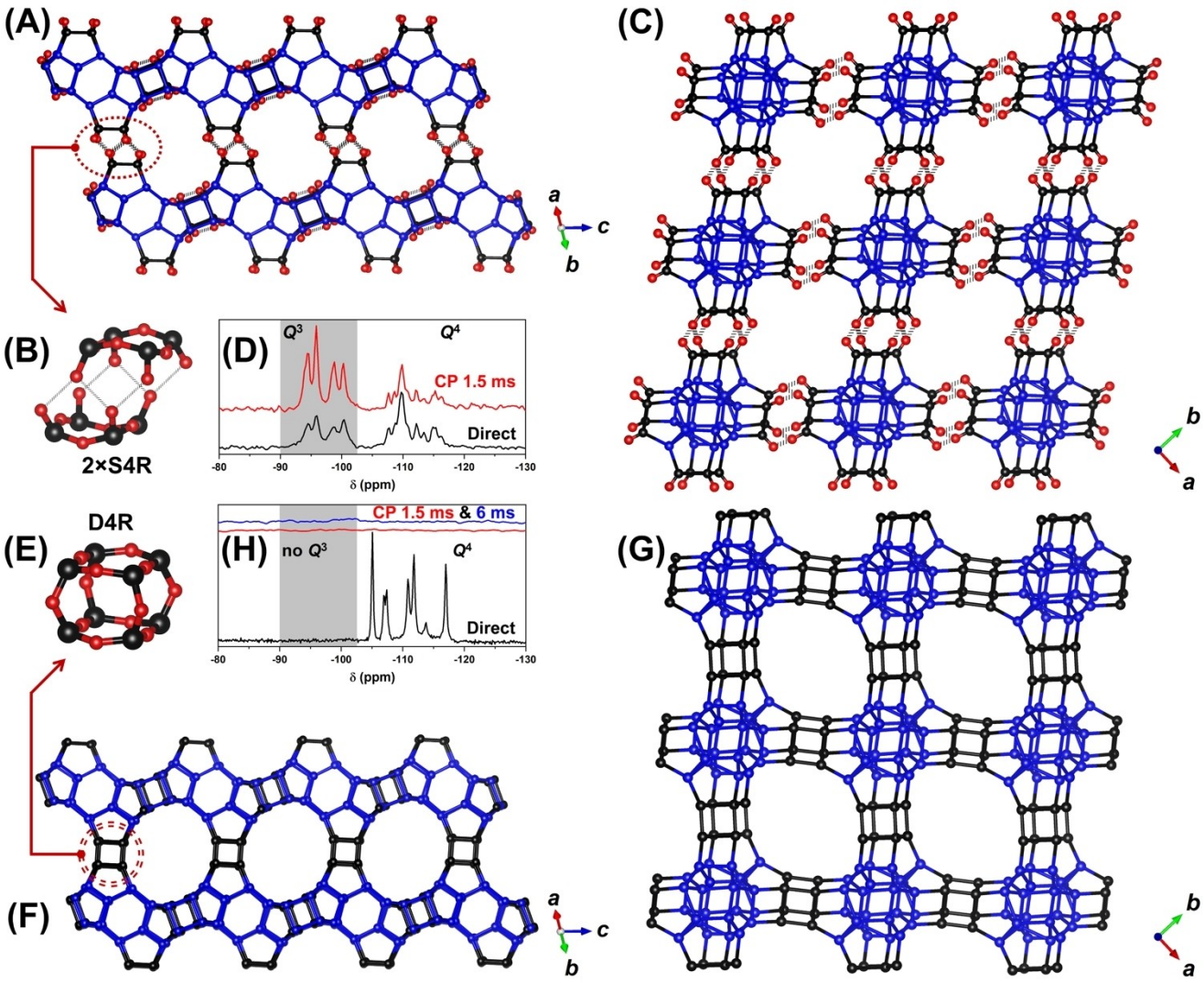

Figure 5. ZEO-2 (top panel) is not a zeolite but a chain silicate (A, C). Neighboring chains are held together by hydrogen bonds between silanols located in *s4r* (B). The existence of Q^4 (blue balls) and Q^3 (black balls) is evident in the ^{29}Si MAS NMR spectra (D) showing a significance enhancement under cross polarization conditions (red trace) compared to direct irradiation (black trace). Only O atoms belonging to silanols are shown (red balls). Upon calcination (bottom panel), condensation of the silanols in *s4r* of ZEO-2 gives rise to *d4r* (E) and the extra-large pore zeolite ZEO-3 with 14R (F) and 16R (G) pores. The transformation is topotactic (the topology of the chain is preserved) and essentially quantitative, as shown by the lack of Q^3 in the ^{29}Si MAS NMR spectra (H). Modified from reference[46] with permission, copyright © 2023 The American Association for the Advancement of Science.

more structural parameters,[69] predicted two ^{29}Si chemical shift ranges for ZEO-5: −94/-97 ppm for the Si in the central *t4r* ring and −103/−117 ppm for the rest of Si.

It is possible to incorporate Ti into ZEO-5 by reaction with $TiCl_4$ vapour at 300 °C. The resulting Ti-ZEO-5 is a catalyst for the selective oxidation of organic compounds that performs similarly to the large pore Ti-Beta when the size of reactants is not very large and much better when it is. It shows potential for the epoxidation of propene with cumene hydroperoxide, with a better performance than the standard mesoporous Ti-HMS catalyst (Figures 4B–C).[70] This better performance despite a smaller pore emphasizes the typical advantage of a higher intrinsic activity of crystalline zeolites versus mesoporous materials.

4. Remarks and future prospects

The 3D ELP zeolites discussed in Section 3 represent a significant leap forward compared to those in Section 2. They hold record breaking porosity, a high stability and an improved performance and competitivity compared to prior zeolites, both as adsorbents for pollution abatement and as catalysts for the petrochemical and fine chemistry industries. ZEO-1 outperforms **FAU** in the adsorption of large dyes and ZEO-3 shows a higher adsorption capacity and a lower desorption temperature than zeolite beta in the removal and recovery of VOC. It also shows a better stability than UiO-66, which degrades rapidly despite the relatively mild conditions of that process. Additionally, aluminosilicate ZEO-1 shows a higher conversion in the catalytic cracking

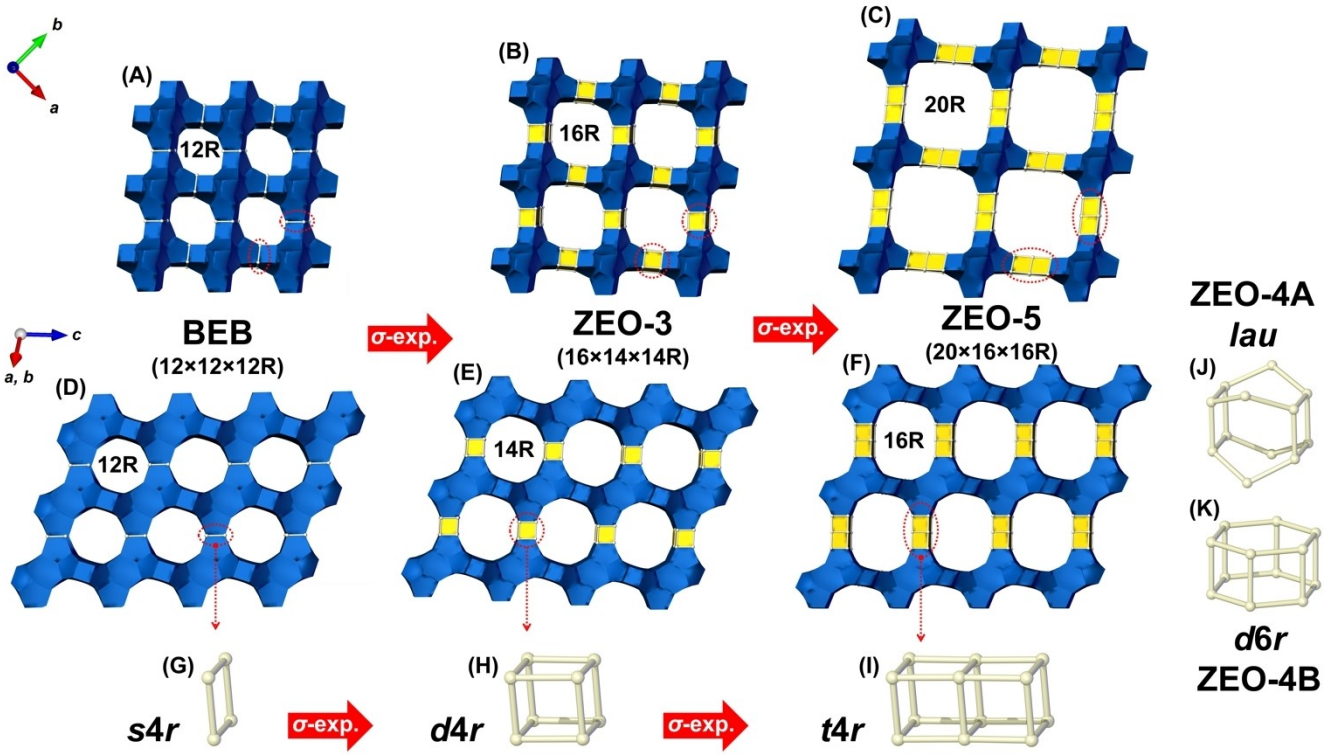

Figure 6. The chain silicate ZEO-2 is embedded into polymorph B of large pore (A, D) zeolite Beta (left) with sharing of *s4r* between adjacent chains. A σ-expansion along two planes transform the *s4r* (G) into *d4r* (H) and the large 12R pores into extra-large 16R (B) and 14R (E) pores in zeolite ZEO-3. A further σ-expansion converts the *d4r* into *t4r* (I) and the extra-large 16R and 14R pores into the larger 20R (C) and 16R (F) pores of ZEO-5. While the first σ-expansion is merely formal, the second one is real since new Si atoms were introduced by silylation in between the s4r to produce the intermediate ZEO-4A (J) and ZEO-4B (K) whose *lau* or *d6r* units condense into the *t4r* of ZEO-5 through a topotactic condensation. Reproduced from reference[47].

of heavy oil, with higher yields of valuable commodities and fuels, hence providing a way for a better use of resources. On its side, titanosilicate ZEO-5, despite being microporous, outperforms mesoporous materials yielding more propylene oxide in the PO-only CHPO reaction, indicating a higher intrinsic activity of the zeolite catalytic centers.

These three zeolites ZEO-1, ZEO-3 and ZEO-5 not only establish three new porosity records and demonstrate the advantages of 3D ELP in applications and the high stability of true, fully connected silica zeolites. They also enlighten some interesting points regarding the concept of feasibility and preparation techniques. First, considering that ZEO-3 and ZEO-5 contain structural units (fluoride free *d4r* and *t4r*, respectively) that can be considered strained and possibly unattainable by direct conventional hydrothermal routes, their preparation by a 1D-to-3D topotactic condensation or by an interchain expansion zeolite reaction followed by condensation, respectively, show how unconventional synthesis routes may produce unconventional materials that might be unreachable by a conventional synthesis,[64] while still allowing the introduction of active centers. This builds upon previous similar conclusions resulting from the preparation of zeolites considered unfeasible through the ADOR process,[71] or by the use of fluoride in the synthesis.[72] In addition, here we propose that unstable materials frequently encountered in the search for new zeolites and dismissed out of hand because of their instability should be reconsidered and their structures solved, as they could be chain or lamellar silicates susceptible to unconventional transformations such as those examined here. Given the power of the new electron diffraction methods commented above, this seems a sensible avenue for future developments.

Secondly, with respect to the preparation of ZEO-1, our results suggest that testing higher crystallization temperatures than usual can be an interesting strategy when an OSDA "does not work", since it can allow to obtain materials whose crystallization present high activation energies. It also shows that this higher temperature and longer reaction time do not necessarily lead to higher density and more thermodynamically stable phases (such as quartz), as might be expected. This strategy is, of course, conditioned on a good thermal stability of the OSDA and in this respect more work should probably be done with phosphonium cations. Actually, given that in the $AlPO_4$ system odd-membered rings are prevented, research with the phosphonium cation used to prepare ZEO-1 and ZEO-2 (both containing 5-rings) but for $AlPO_4$ compositions might produce interesting new high porosity molecular sieves.

The works reviewed here also highlight that, while machine learning and artificial intelligence will eventually dictate how to discover new zeolites,[73] trial and error

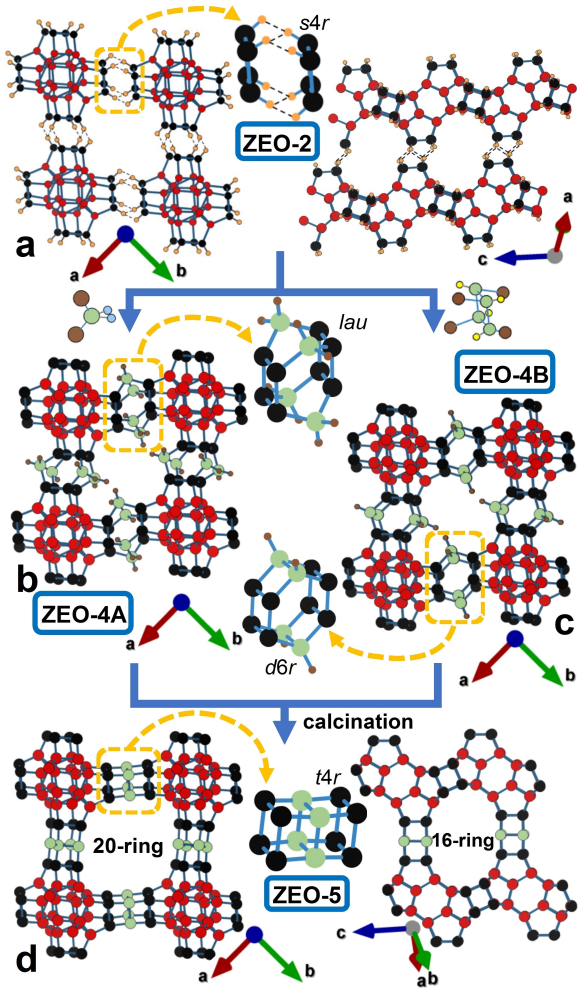

Figure 7. The Interchain Expansion Zeolite reaction. Silylation of the chain silicate ZEO-2 (a) with either DCDMS or TMCTS produce the expanded interrupted materials ZEO-4A (b) and -4B (c), respectively. They differ in the way the chains are linked together through *lau* or *d6r* units, respectively. Calcination of both materials produce the same fully connected true zeolite, ZEO-5 (d), featuring a *t4r* unit and 20R and 16R extra-large pores. Reproduced from reference[47].

guided by the empirical wealth of information accumulated in over 80 years is still worth trying.

In contrast to the meager success of earlier efforts of searching for more porous zeolites, these recent advances suggest the scenario might rapidly change. Since the three new materials demonstrate stable 3D ELP zeolites are indeed possible and present significant advantages in catalytic and adsorption processes, this should encourage further research in this field. In fact, when this work was under peer review we got notice of a new stable ELP zeolite, ZMQ-1, which for the first time ever in zeolites reaches the mesopore regime along one direction (28R) although it only has medium pores in the other directions (i.e., 3D 28x10x10).[74] We have no information on its synthesis but this new ELP zeolite, together with the materials reviewed here, demonstrate that the limit of porosity in zeolites had not been reached and that this field of research is now currently in the spotlight.[74]

Acknowledgements

Financial support from the Spanish Ministry of Science Innovation (PID2022-137889OB–I00, PID2021-128141OB–C22, TED2021-131223B–I00, MCIN/AEI/10.13039/501100011033), and Generalitat Valenciana (PROMETEO CIPROM/2021/007) are gratefully acknowledged. H.Y. is grateful to the China Scholarship Council for a PhD grant.

Conflict of Interest

ZRG have filled a patent on ZEO-1, ZEO-2 and ZEO-3.

Data Availability Statement

Data sharing is not applicable to this article as no new data were created or analyzed in this study.

Keywords: Extra-large Pores · Zeolites · Porosity · Stability · Application

[1] C. Baerlocher, L. B. McCusker, Database of Zeolite Structures, http://www.iza-structure.org/databases/, May 20 2024.
[2] A. K. Cheetham, G. Férey, T. Loiseau, *Angew. Chem. Int. Ed.* **1999**, *38*, 3268–3292.
[3] a) J. G. Min, K. C. Kemp, S. B. Hong, *Sep. Purif. Technol.* **2020**, *250*, 117146; b) K. Chen, S. H. Mousavi, R. Singh, R. Q. Snurr, G. Li, P. A. Webley, *Chem. Soc. Rev.* **2022**, *51*, 1139–1166; c) C. Chizallet, C. Bouchy, K. Larmier, G. Pirngruber, *Chem. Rev.* **2023**, *123*, 6107–6196; d) J. Shin, D. S. Bhange, M. A. Camblor, Y. Lee, W. J. Kim, I.-S. Nam, S. B. Hong, *J. Am. Chem. Soc.* **2011**, *133*, 10587–10598; e) R. Bueno-Perez, S. R. G. Balestra, M. A. Camblor, J. G. Min, S. B. Hong, P. J. Merkling, S. Calero, *Chem. Eur. J.* **2018**, *24*, 4121–4132; f) M. E. Medina, A. E. Platero-Prats, N. Snejko, A. Rojas, A. Monge, F. Gándara, E. Gutiérrez-Puebla, M. A. Camblor, *Adv. Mater.* **2011**, *23*, 5283–5292; g) S. Li, H. Yang, S. Wang, J. Wang, W. Fan, M. Dong, *Chem. Comm.* **2022**, *58*, 2041–2054; h) S. C. Larsen, *J. Phys. Chem. C* **2007**, *111*, 18464–18474.
[4] a) D. Kalló, *RIMG* **2001**, *45*, 519–550; b) E. Koohsaryan, M. Anbia, M. Maghsoodlu, *J. Environ. Chem. Eng.* **2020**, *8*, 104287.
[5] a) S. Rossini, *Catal. Today* **2003**, *77*, 467–484; b) T. F. Degnan, *Top. Catal.* **2000**, *13*, 349–356; c) T.-Y. Cui, A. Rajendran, H.-X. Fan, J. Feng, W.-Y. Li, *Ind. Eng. Chem. Res.* **2021**, *60*, 3295–3323.
[6] a) Y. Wu, B. M. Weckhuysen, *Angew. Chem. Int. Ed.* **2021**, *60*, 18930–18949; b) D. Fu, M. E. Davis, *Chem. Soc. Rev.* **2022**, *51*, 9340–9370; c) A. Mehdikhani, E. Salahi, J. Shahmoradi, *Adsorption* **2024**, 1–7.
[7] L. Gómez-Hortigüela, J. Pérez-Pariente, Y. Chebude, I. Díaz, *RSC Adv.* **2014**, *4*, 7998–8003.
[8] a) W. Vermeiren, J.-P. Gilson, *Top. Catal.* **2009**, *52*, 1131–1161; b) M. Zaarour, B. Dong, I. Naydenova, R. Retoux, S. Mintova, *Microporous and Mesoporous Materials* **2014**, *189*, 11–21.
[9] E. M. Flanigen, *Stud. Surf. Sci. Catal.* **1991**, *58*, 13–34.
[10] M. E. Davis, *Nature* **1989**, *337*, 117.
[11] C. Perego, R. Millini, *Chem. Soc. Rev.* **2013**, *42*, 3956–3976.

[12] J. Liang, Z. Liang, R. Zou, Y. Zhao, *Adv. Mater.* **2017**, *29*, 1701139.
[13] D. Wikoff, L. Fitzgerald, L. Birnbaum, in *Dioxins and Health: Including Other Persistent Organic Pollutants and Endocrine Disruptors*, John Wiley & Sons, Inc., **2012**, pp. 1–36.
[14] C. S. Cundy, P. A. Cox, *Chem. Rev.* **2003**, *103*, 663–702.
[15] M. E. Davis, C. Saldarriaga, C. Montes, J. Garces, C. Crowdert, *Nature* **1988**, *331*, 698–699.
[16] R. M. Dessau, J. L. Schlenker, J. B. Higgins, *Zeolites* **1990**, *10*, 522–524.
[17] M. Estermann, L. B. McCusker, C. Baerlocher, A. Merrouche, H. Kessler, *Nature* **1991**, *352*, 320–323.
[18] C. C. Freyhardt, M. Tsapatsis, R. F. Lobo, K. J. Balkus, M. E. Davis, *Nature* **1996**, *381*, 295–298.
[19] P. Wagner, M. Yoshikawa, M. Lovallo, K. Tsuji, M. Taspatsis, M. E. Davis, *Chem. Comm.* **1997**, 2179–2180.
[20] A. K. Cheetham, H. Fjellvag, T. E. Gier, K. O. Kongshaug, K. P. Lillerud, G. D. Stucky, *Stud. Surf. Sci. Catal.* **2001**, *135*, 158.
[21] K. G. Strohmaier, D. E. W. Vaughan, *J. Am. Chem. Soc.* **2003**, *125*, 16035–16039.
[22] A. Burton, S. Elomari, C.-Y. Chen, R. C. Medrud, I. Y. Chan, L. M. Bull, C. Kibby, T. V. Harris, S. I. Zones, E. S. Vittoratos, *Chem. Eur. J.* **2003**, *9*, 5737–5748.
[23] J.-L. Paillaud, B. Harbuzaru, J. Patarin, N. Bats, *Science* **2004**, *304*, 990–992.
[24] A. Corma, M. J. Díaz-Cabañas, J. L. Jordá, C. Martínez, M. Moliner, *Nature* **2006**, *443*, 842–845.
[25] J. Sun, C. Bonneau, Á. Cantín, A. Corma, M. J. Díaz-Cabañas, M. Moliner, D. Zhang, M. Li, X. Zou, *Nature* **2009**, *458*, 1154–1157.
[26] J. Jiang, J. L. Jorda, M. J. Diaz-Cabanas, J. Yu, A. Corma, *Angew. Chem. Int. Ed.* **2010**, *49*, 4986–4988.
[27] A. Corma, M. J. Díaz-Cabañas, J. Jiang, M. Afeworki, D. L. Dorset, S. L. Soled, K. G. Strohmaier, *PNAS* **2010**, *107*, 13997–14002.
[28] J. Jiang, J. L. Jorda, J. Yu, L. A. Baumes, E. Mugnaioli, M. J. Diaz-Cabanas, U. Kolb, A. Corma, *Science* **2011**, *333*, 1131–1134.
[29] R. Martínez-Franco, M. Moliner, Y. Yun, J. Sun, W. Wan, X. Zou, A. Corma, *PNAS* **2013**, *110*, 3749–3754.
[30] T. Willhammar, A. W. Burton, Y. Yun, J. Sun, M. Afeworki, K. G. Strohmaier, H. Vroman, X. Zou, *J. Am. Chem. Soc.* **2014**, *136*, 13570–13573.
[31] F.-J. Chen, Y. Xu, H.-B. Du, *Angew. Chem. Int. Ed.* **2014**, *53*, 9592–9596.
[32] S. Smeets, D. Xie, C. Baerlocher, L. B. McCusker, W. Wan, X. Zou, S. I. Zones, *Angew. Chem. Int. Ed.* **2014**, *53*, 10398–10402.
[33] J. Jiang, Y. Yun, X. Zou, J. L. Jorda, A. Corma, *Chem. Sci.* **2015**, *6*, 480–485.
[34] C. Jo, S. Lee, S. J. Cho, R. Ryoo, *Angew. Chem. Int. Ed.* **2015**, *54*, 12805–12808.
[35] Y. Yun, M. Hernández, W. Wan, X. Zou, J. L. Jordá, A. Cantín, F. Rey, A. Corma, *Chem. Comm.* **2015**, *51*, 7602–7605.
[36] J. H. Kang, D. Xie, S. I. Zones, S. Smeets, L. B. McCusker, M. E. Davis, *Chem. Mater.* **2016**, *28*, 6250–6259.
[37] C. Zhang, E. Kapaca, J. Li, Y. Liu, X. Yi, A. Zheng, X. Zou, J. Jiang, J. Yu, *Angew. Chem. Int. Ed.* **2018**, *57*, 6486–6490.
[38] B. Yang, J.-G. Jiang, H. Xu, H. Wu, M. He, P. Wu, *Angew. Chem. Int. Ed.* **2018**, *57*, 9515–9519.
[39] W.-W. Zi, Z. Gao, J. Zhang, B.-X. Zhao, X.-S. Cai, H.-B. Du, F.-J. Chen, *Angew. Chem. Int. Ed.* **2020**, *59*, 3948–3951.
[40] L. A. Villaescusa, J. Li, Z. Gao, J. Sun, M. A. Camblor, *Angew. Chem. Int. Ed.* **2020**, *59*, 11283–11286.
[41] Z. R. Gao, J. Li, C. Lin, A. Mayoral, J. Sun, M. A. Camblor, *Angew. Chem. Int. Ed.* **2021**, *60*, 3438–3442.
[42] E. Kapaca, J. Jiang, J. Cho, J. L. Jordá, M. J. Díaz-Cabañas, X. Zou, A. Corma, T. Willhammar, *J. Am. Chem. Soc.* **2021**, *143*, 8713–8719.
[43] Q.-F. Lin, Z. R. Gao, C. Lin, S. Zhang, J. Chen, Z. Li, X. Liu, W. Fan, J. Li, X. Chen, M. A. Camblor, F.-J. Chen, *Science* **2021**, *374*, 1605–1608.
[44] X. Cai, Y. Zhao, W. Zi, F. Jiao, H. Du, *Chem. Eur. J.* **2022**, *28*, e202200934.
[45] A. Sala Gascón, Dissertation, Universitat Politècnica de València **2022**.
[46] J. Li, Z. R. Gao, Q.-F. Lin, C. Liu, F. Gao, C. Lin, S. Zhang, H. Deng, A. Mayoral, W. Fan, S. Luo, X. Chen, H. He, M. A. Camblor, F.-J. Chen, J. Yu, *Science* **2023**, *379*, 283–287.
[47] Z. R. Gao, H. Yu, F.-J. Chen, A. Mayoral, Z. Niu, Z. Niu, X. Li, H. Deng, C. Márquez-Álvarez, H. He, S. Xu, Y. Zhou, J. Xu, H. Xu, W. Fan, S. R. G. Balestra, C. Ma, J. Hao, J. Li, P. Wu, J. Yu, M. A. Camblor, *Nature* **2024**, *628*, 99–103.
[48] Y. Luo, H. Xu, Y. Han, W. Tong, M. Jiao, N. Wang, J. Jiang, X. Zou, P. Wu, *ChemRXiv preprint* **2024**, DOI: 10.26434/chemrxiv-2023-pdtg4-v2.
[49] E. R. Parnham, R. E. Morris, *Acc. Chem. Res.* **2007**, *40*, 1005–1013.
[50] V. R. R. Marthala, M. Hunger, F. Kettner, H. Krautscheid, C. Chmelik, J. Kärger, J. Weitkamp, *Chem. Mater.* **2011**, *23*, 2521–2528.
[51] Q. Wu, X. Liu, L. Zhu, L. Ding, P. Gao, X. Wang, S. Pan, C. Bian, X. Meng, J. Xu, F. Deng, S. Maurer, U. Müller, F.-S. Xiao, *J. Am. Chem. Soc.* **2015**, *137*, 1052–1055.
[52] T. Blasco, A. Corma, M. J. Díaz-Cabañas, F. Rey, J. A. Vidal-Moya, C. M. Zicovich-Wilson, *J. Phys. Chem. B* **2002**, *106*, 2634–2642.
[53] L. A. Villaescusa, P. A. Barrett, M. A. Camblor, *Angew. Chem. Int. Ed.* **1999**, *38*, 1997–2000.
[54] G. O. Bnmner, W. M. Meier, *Nature* **1989**, *337*, 146–147.
[55] L. A. Villaescusa, M. A. Camblor, *Chem. Mater.* **2016**, *28*, 7544–7550.
[56] O. Veselý, R. E. Morris, J. Čejka, *Microporous Mesoporous Mater.* **2023**, *358*, 112385.
[57] L. Burel, N. Kasian, A. Tuel, *Angew. Chem. Int. Ed.* **2014**, *53*, 1360–1363.
[58] W. J. Roth, P. Nachtigall, R. E. Morris, P. S. Wheatley, V. R. Seymour, S. E. Ashbrook, P. Chlubná, L. Grajciar, M. Položij, A. Zukal, O. Shvets, J. Čejka, *Nat. Chem* **2013**, *5*, 628–633.
[59] a) P. S. Wheatley, P. Chlubná-Eliášová, H. Greer, W. Zhou, V. R. Seymour, D. M. Dawson, S. E. Ashbrook, A. B. Pinar, L. B. McCusker, M. Opanasenko, J. Čejka, R. E. Morris, *Angew. Chem. Int. Ed.* **2014**, *53*, 13210–13214; b) O. Veselý, P. Eliášová, R. E. Morris, J. Čejka, *Mater. Adv.* **2021**, *2*, 3862–3870.
[60] J. Simancas Coloma, Dissertation, Universitat Politècnica de València, Spain, 2021.
[61] M. E. Davis, R. F. Lobo, *Chem. Mater.* **1992**, *4*, 756–768.
[62] M. Fahda, J. Fayek, E. Dib, H. Cruchade, N. Pichot, N. Chaouati, L. Pinard, P. S. Petkov, G. N. Vayssilov, A. Mayoral, B. Witulski, L. Lakiss, V. Valtchev, *Chem. Mater.* **2024**, *36*, 5405–5421.
[63] J. M. Newsam, M. M. J. Treacy, W. T. Koetsier, C. B. D. Gruyter, *Proc. R. Soc. Lond. A* **1988**, *420*, 375–405.
[64] R. E. Morris, *Science* **2023**, *379*, 236–237.
[65] C. M. Zicovich-Wilson, M. L. San-Román, M. A. Camblor, F. Pascale, J. S. Durand-Niconoff, *J. Am. Chem. Soc.* **2007**, *129*, 11512–11523.
[66] W. Fan, P. Wu, S. Namba, T. Tatsumi, *J. Catal.* **2006**, *243*, 183–191.
[67] R. Pophale, P. A. Cheeseman, M. W. Deem, *Phys. Chem. Chem. Phys.* **2011**, *13*, 12407–12412.

[68] J. M. Thomas, J. Klinowski, S. Ramdas, B. K. Hunter, D. T. B. Tennakoon, *Chem. Phys. Lett.* **1983**, *102*, 158–162.
[69] D. M. Dawson, R. F. Moran, S. E. Ashbrook, *J. Phys. Chem. C* **2017**, *121*, 15198–15210.
[70] L. Xu, H. Liu, *Propylene Epoxidation with Cumene Hydroperoxide/Titanosilicates, in Micro-Mesoporous Metallosilicates*, John Wiley & Sons, Ltd, **2024**, pp. 345–366.
[71] M. Mazur, P. S. Wheatley, M. Navarro, W. J. Roth, M. Položij, A. Mayoral, P. Eliášová, P. Nachtigall, J. Čejka, R. E. Morris, *Nat. Chem* **2016**, *8*, 58–62.
[72] A. Rojas, M. A. Camblor, *Angew. Chem. Int. Ed.* **2012**, *51*, 3854–3856.
[73] F. Daeyaert, M. W. Deem, *ChemistrySelect* **2019**, *4*, 3531–3537.
[74] V. Valtchev, The quest for extra-large pore zeolites: Where is the limit? in ZMPC International Symposium on Zeolites and MicroPorous Crystals, Osaka, Japan, July 21–25, 2024.

Manuscript received: June 28, 2024
Revised manuscript received: August 9, 2024
Accepted manuscript online: August 14, 2024
Version of record online: October 4, 2024